MEASURING THE INTRINSIC DIMENSION OF OBJECTIVE LANDSCAPES

Anonymous authors
Paper under double-blind review

ABSTRACT

Many recently trained neural networks employ tens or hundreds of millions of parameters to achieve good performance. Researchers may intuitively use the number of parameters required as a rough gauge of the difficulty of a problem. But how accurate are such notions? How many parameters are really needed? In this paper we attempt to answer this question by training networks not in their native parameter space, but instead in smaller, randomly oriented subspaces. By slowly increasing the dimension of this subspace, we note when solutions first appear and define this to be the *intrinsic dimension* of the problem. A few suggestive conclusions result. Many problems have smaller intrinsic dimension than one might suspect, and the intrinsic dimension for a given dataset varies little across a family of models with vastly different sizes. Intrinsic dimension allows some quantitative problem comparison across supervised, reinforcement, and other types of learning where we conclude, for example, that solving the cart-pole RL problem is in a sense 100 times easier than classifying digits from MNIST. In addition to providing new cartography of the objective landscapes wandered by parameterized models, the results encompass a simple method for constructively obtaining an upper bound on the minimum description length of a solution, leading in some cases to very compressible networks.

1 INTRODUCTION

In this paper we define and investigate the *intrinsic dimension* of neural network optimization problems. To introduce this concept, we first briefly review neural network training from an optimization perspective.

Training a neural network to model a given dataset entails several steps. First, a network designer chooses a loss and a network architecture. The architecture is then initialized by populating its weights with random values drawn from some distribution. Finally the network is trained, during which weights are adjusted to produce a loss for the dataset that is as low as possible.

We can think of the training procedure as traversing some path along an *objective landscape*. Note that as soon as a dataset, loss, and network architecture are specified, the landscape in its entirety is completely determined. It is instantiated and frozen; all subsequent parameter initialization, forward prop, back prop, gradients, and steps determined and taken by some optimizer are just details of how one explores this fixed space.

Consider a network parameterized by D weights. We can picture the associated objective landscape as a set of hills and valleys in D dimensions, where each point in $\mathbb{R}^D$ corresponds to a value of the loss, or the elevation of landscape above (or below) 0. If D were two, the map from two coordinates to one is easily imagined and intuitively understood by those living in a three-dimensional world with similar hills. However, in higher dimensions, our intuitions are not so faithful, and generally we should be careful as extrapolating from low-dimensional intuitions to higher-dimensions can lead to unreliable conclusions. The difficulty of imagining and understanding high-dimensional objective landscapes notwithstanding, it is the lot of neural network researchers to spend their days leading (or following?) networks over these multi-dimensional surfaces, so any reported and interpreted geography of these landscapes should be valuable.

Several papers have shed valuable light on this landscape, particularly by pointing out flaws in our extrapolation from low-dimensional reasoning. Dauphin et al. (2014) showed that, in contrast to conventional thinking about getting stuck in local optima (as one might be stuck in a valley in our familiar $D = 2$), local critical points in high dimension are almost never valleys but are instead saddlepoints: structures which are "valleys" along a multitude of dimensions with "exits" in a multitude of other dimensions. The striking conclusion is that one has less to fear becoming hemmed in on all sides by higher loss but more to fear being waylaid nearly indefinitely by nearly flat regions. Goodfellow et al. (2015) showed another property: that paths directly from the initial point to the final point of optimization are often monotonically decreasing. Though dimension is high, the space is in some sense simpler than we thought: rather than winding around hills and through long twisting corridors, the walk could just as well have taken a straight line without encountering any obstacles, if only the direction of the line could have been determined at the outset.

In this paper we seek further understanding of the structure of the objective landscape by restricting training to random slices through it, allowing optimization to proceed in randomly generated subspaces of the full parameter space. Whereas standard neural network training involves computing a gradient and taking a step in the full parameter space ($\mathbb{R}^D$ above), we instead choose a random d-dimensional subspace of $\mathbb{R}^D$, where generally $d < D$, and optimize directly in this subspace. By performing experiments with gradually larger values of d, we can find the subspace dimension at which solutions first appear, which we call the measured *intrinsic dimension* of a particular problem. Examining intrinsic dimensions across a variety of problems leads to a few new intuitions about the optimization problems that arise from neural network models. We begin by defining more precisely the notion of intrinsic dimension.

2 Defining and Approximating Intrinsic Dimension

We introduce the intrinsic dimension of an objective landscape by way of an illustrative toy problem. Let D be the dimension of a parameter space, $\theta^{(D)} \in \mathbb{R}^D$ a parameter vector in that space, $\theta_0^{(D)}$ a randomly chosen initial parameter vector, and $\theta_*^{(D)}$ the final parameter vector arrived at via optimization.

Consider a toy optimization problem where $D = 1000$, $\theta_0^{(D)}$ is drawn from a Gaussian distribution, and then $\theta^{(D)}$ optimized to minimize a squared error cost function that requires the first 100 elements to sum to 1, the second 100 elements to sum to 2, and so on until the vector has been divided into 10 groups with their requisite 10 sums. We may use optimization to easily find a $\theta_*^{(D)}$ that solves the problem with zero cost.

Solutions to this problem are highly redundant. With a little algebra one can find that the manifold of solutions is a 990 dimensional hyperplane: from any point that has zero cost, there are 990 orthogonal directions one can move and remain at zero cost. Denoting as s the dimensionality of the solution set, we define the intrinsic dimensionality d_{int} of a solution as the codimension of the solution set inside of $\mathbb{R}^D$:

$$D = d_{\text{int}} + s \tag{1}$$

Here the intrinsic dimension d_{int} is 10 (1000 = 10 + 990), with 10 corresponding intuitively to the number of constraints placed on the parameter vector.

2.1 Measuring Intrinsic Dimension via Random Subspace Training

The above example had simple enough form that we obtained $d_{\text{int}} = 10$ by calculation, but in general, we desire a method of measuring or approximating d_{int} for more complicated problems, including problems with data dependent objective functions. We find such a method in random subspace optimization.

Standard optimization, which we will refer to hereafter as the *direct* method of training, entails evaluating the gradient of a loss with respect to $\theta^{(D)}$ and taking steps directly in the space of $\theta^{(D)}$. To train in a random subspace, we instead define $\theta^{(D)}$ in the following way:

$$\theta^{(D)} = \theta_0^{(D)} + P\theta^{(d)} \tag{2}$$

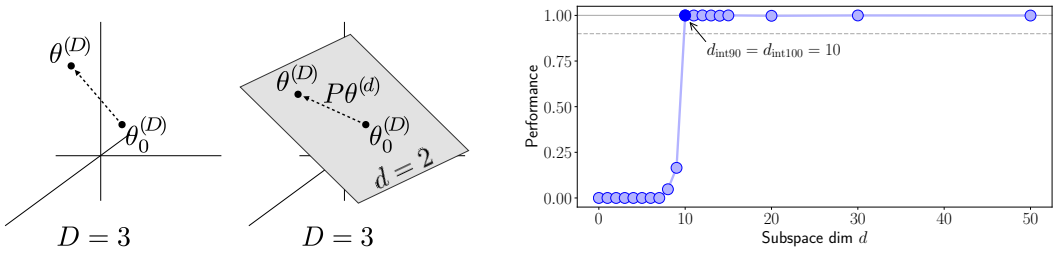

Figure 1: **(left)** Illustration of parameter vectors for direct optimization in the $D = 3$ case. **(middle)** Illustration of parameter vectors and a possible random subspace for the $D = 3, d = 2$ case. **(right)** Plot of performance vs. subspace dimension for the toy example of toy example of Sec. 2. The problem becomes 90% solvable and 100% solvable at random subspace dimension 10, so d_{int90} and d_{int100} are 10.

where P is a randomly generated $D \times d$ projection matrix[1] and $\theta^{(d)}$ is a parameter vector in a generally smaller space $\mathbb{R}^d$. $\theta_0^{(D)}$ and P are randomly generated and frozen (not trained), so the system has only d degrees of freedom. We initialize $\theta^{(d)}$ to a vector of all zeros, so initially $\theta^{(D)} = \theta_0^{(D)}$, a setting that serves two related purposes: First, it puts the subspace used for training and the solution set in *general position* with respect to each other. Intuitively, this avoids cases where both the solution set and the random subspace contain structure oriented around the origin, which could lead to non-intersection even for high-dimensional solution sets and random subspaces. Second, in the case of neural network training, it allows the network to benefit from beginning in a region of parameter space supposed by any number of initialization schemes to be well-conditioned (Glorot & Bengio, 2010; He et al., 2015) such that gradient descent via commonly used optimizers tends to produce a $\theta_*^{(D)}$ with low loss. Note that setting $\theta_0^{(D)}$ to an all-zero vector is often an exceptionally poor choice for neural networks: for reasons of symmetry, the gradient can end up being zero in many directions, hindering effective optimization.

Training proceeds by computing gradients with respect to $\theta^{(d)}$ and taking steps in that space. Columns of P are normalized to unit length, so steps of unit length in $\theta^{(d)}$ chart out unit length motions of $\theta^{(D)}$. Columns of P may also be orthogonalized if desired, but in our experiments we relied simply on the approximate orthogonality of high dimensional random vectors. By this construction P forms an approximately orthonormal basis for a randomly oriented d dimensional subspace of $\mathbb{R}^D$, with the origin of the new coordinate system at $\theta_0^{(D)}$. Fig. 1 shows an illustration of the related vectors.

Consider the optimization problem this formulation creates. If we set $d = D$ and make P a large identity matrix, we recover exactly the direct optimization problem. If $d = D$ but P is instead a random orthonormal basis for all of $\mathbb{R}^D$, we recover a rotated version of the direct problem. Note that for some "rotation-invariant" optimizers, such as SGD and SGD with momentum, rotating the basis will not change the solution found, but for optimizers with axis-aligned assumptions, such as RMSProp (Tieleman & Hinton, 2012) or Adam (Kingma & Ba, 2014), the path taken through $\theta^{(D)}$ space by an optimizer will depend on the rotation chosen. Finally, in the general case where $d < D$ and solutions exist in D, solutions will *almost surely* (with probability 1) not be found if d is less than the codimension of the solution but may be found when $d \geq D - s$. If the solution set is a hyperplane, the solution will almost surely intersect the subspace, but in the general case of non-hyperplane solution sets, intersection with a random subspace of dimension d_{int} is not guaranteed. Nonetheless by increasing d and checking for solutions, we obtain one estimate of d_{int}. We try this sweep of d for our toy problem, measuring by convention as described in the next section positive performance instead of loss.[2] As expected and as can be seen in Fig. 1 (right) solutions are first found at $d = 10$.

[1]This projection matrix can take a variety of forms each with different computational considerations. In later sections we consider dense, sparse, and implicit P matrices.

[2]For this toy problem we define $\text{performance} = \exp(-\text{loss})$, bounding performance between 0 and 1, with 1 being a perfect solution.

2.2 DETAILS AND CONVENTIONS

In the rest of this paper, we measure intrinsic dimensions for particular neural network problems and draw conclusions about the associated objective landscapes and solution sets. Because modeling real data is more complex than the above toy example, and losses are generally never exactly zero, we first choose a heuristic for classifying points on the objective landscape as solutions vs. non-solutions. The heuristic we choose is to threshold network performance at the level of some baseline model, where generally we take as baseline the best directly trained model. In supervised classification settings, validation accuracy is used as the measure of performance, and in reinforcement learning scenarios, total reward (shifted up or down such that the minimum reward is 0) is used. Accuracy and reward are preferred to loss to ensure results are grounded to real-world performance and to allow comparison across models with differing scales of loss and different amounts of regularization included in the loss.

We define d_{int100} as the intrinsic dimension of the "100%" solution: those solutions whose performance is statistically indistinguishable from direct, baseline solutions. However, we observed these to vary widely and for a few confounding reasons: d_{int100} can be very high — nearly as high as D — when the task requires matching a very well-tuned baseline model but can drop significantly when the regularizing effect of restricting parameters to a subspace boosts performance by tiny amounts. While these are interesting effects, we primarily set out to measure the basic difficulty of problems and the degrees of freedom needed to solve (or approximately solve) them rather than these second order effects.

Thus, we found it more useful to define and measure d_{int90} as the intrinsic dimension of the "90%" solution: those with performance at least 90% of the baseline. We chose 90% after looking at a variety of dimension vs. performance plots as a reasonable trade off between wanting to guarantee the solution found is as good as possible, but also not wanting measured d values to be very sensitive to small noise in measured performance. If too high a threshold is used, then the point of crossing the threshold changes a lot for only tiny changes in accuracy, and we always observe tiny changes in accuracy due to training noise. If a higher (or lower) threshold were chosen, we expect most of results in the rest of the paper to remain qualitatively unchanged, albeit with d scaled up (or down) by some factor and more noisily (or less noisily) measured.

3 RESULTS AND DISCUSSION

3.1 MNIST

We begin by analyzing a fully connected (FC) classifier trained on MNIST. We choose a network with two hidden layers of width 400, giving a total number of parameters and thus dimension D of 199,210. Performance vs. subspace dimension d is shown in Fig. 2. By checking the subspace dimension at which performance crosses the 90% mark, we measure this network's intrinsic dimension d_{int90} at about 750.

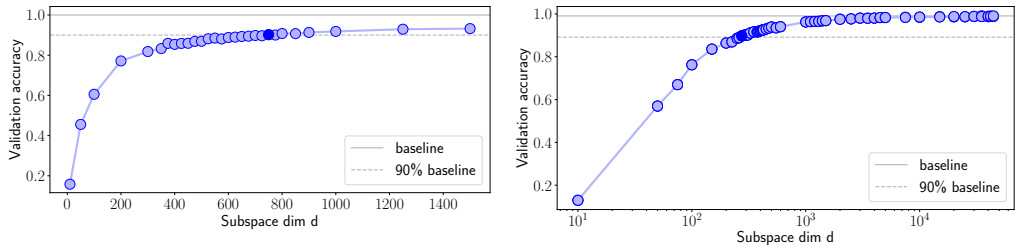

Figure 2: Performance (validation accuracy) vs. subspace dimension d for two networks trained on MNIST: **(left)** a 784-400-400-10 fully-connected (FC) network (D = 199,210) and **(right)** a convolutional network, LeNet (D = 44,426). The solid line shows performance of a well-trained direct (FC or conv) model, and the dashed line shows the 90% threshold we use to define d_{int90}. We oversample the region around the threshold in order to estimate the point of crossing more exactly.

Some networks are very compressible Perhaps the most salient initial conclusion is that 750 is quite low. At that subspace dimension, only 750 degrees of freedom (0.4%) are being used and 198,460 (99.6%) unused to obtain 90% of the performance of the direct baseline model. A compelling corollary of this result is a new way of creating and training compressed networks. To store this network, one need only store the random seed used to generate $\theta_0^{(D)}$ and P and the 750 floating point numbers in $\theta_*^{(d)}$, a compression from 793kB (assuming 32-bit floats) to only 3.2kB or 0.4% of the full parameter size. Such compression could be very useful for including networks in app downloads or on web pages or in other scenarios where storage or bandwidth are limited.

While is has previously been appreciated that large nets waste parameters (Dauphin & Bengio, 2013) and in general weights contain redundancy (Denil et al., 2013), this approach to compression constitutes a much simpler, end-to-end approach applicable to any parameterized model. Our method is different from previous neural networks compression methods in following aspects: *i*) Unlike post-hoc compression (Wen et al., 2016), we train once, end-to-end, and any parameterized model is an allowable base model. *ii*) Compared to methods like that of Louizos et al. (2017), who take a Bayesian perspective and consider redundancy on the level of groups of parameters (input weights to a single neuron) by using group-sparsity-inducing hierarchical priors on the weights, our approach is simpler but not likely to lead to the levels of compression that they attain. *iii*) Compression is achieved in different spaces: previous methods reduce trainable variable directly in the layer-wise parameter spaces: Wen et al. (2016) used layer-wise low rank approximations to the weight matrices, and Han et al. (2016) proposed to prune the weights. We optimize by globally compressing parameter space. *iv*) Finally, there is a beautiful array of papers on compressing networks such that they also achieve computational savings during the forward pass (Wen et al., 2016; Han et al., 2016; Yang et al., 2015); subspace training does not speed up execution time during inference at all.

Robustness of intrinsic dimension Next, we ask how intrinsic dimension varies across FC networks of varying number of layers and varying layer width. Fig. S6 in the Supplementary Information shows performance vs. subspace dimension plots in the style of Fig. 2 for a grid search of networks with number of hidden layers L chosen from $\{1, 2, 3, 4, 5\}$ and width of each hidden layer W chosen from $\{50, 100, 200, 400\}$. All curves are nearly identical! The intrinsic dimension changes little even as models grown in width or depth, indicating that as every extra dimension is added in D, they just end up adding a dimension to the redundancy of the solution. Often the most accurate directly trained models for a problem have far more parameters than needed (Zhang et al., 2017); this may be because they are just easier to train, and our observation suggests a reason why: with larger models, solutions have greater redundancy and in a sense "cover" more of the space. The very similar d_{int90} values for all 20 networks are shown in Fig. 3 plotted against the native dimension D of each network; as one can see, D changes by a factor of 24.1 between the smallest and largest networks, but d_{int90} changes over this range by a factor of only 1.33. Note that for this experiment, we used (90% of) a global 100% baseline, to compare simply and fairly across all models.[3]

Are random subspaces really more parameter-efficient for FC nets? One might wonder to what extent claiming 750 parameters is meaningful given that performance achieved is far lower than a state of the art network trained on MNIST. With such a low bar for performance, could a directly trained network with a comparable number of parameters be found that exhibits the same performance? We generated 1000 smaller networks (depth randomly chosen from $\{1, 2, 3, 4, 5\}$ and layer width from $\{2, 3, 5, 8, 10, 15, 20, 25\}$) in an attempt to find high-performing small FC networks, but as Fig. 4 (left) shows, a $10\times$ gap still exists between the subspace dimension and the smallest direct FC network showing 90% of baseline performance.

Measuring d_{int90} on a convolutional network We measure also d_{int90} of a convolutional network, LeNet (D=44,426), showing validation accuracy vs. subspace dimension d results in Fig. 2 (right). We find $d_{\text{int90}} = 275$, or a compression rate to 0.5%. As with the FC case above, we also do a sweep of random networks, but here find a different story: there is sometimes, but not always, a gap in number of degrees of freedom between convnets and convents trained in a random subspace. We interpret these results in terms of the Minimum Description Length below.

[3]See Sec. S5 for similar results obtained using instead 20 separate baselines for each of the 20 models.

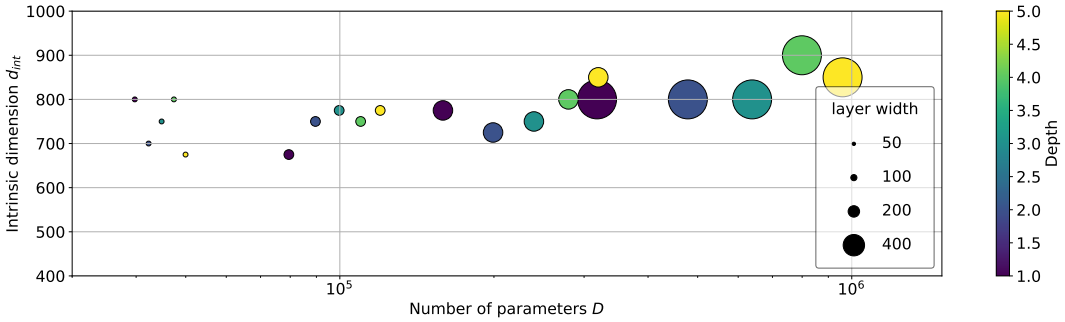

Figure 3: Measured intrinsic dimension d_{int90} vs number of parameters D for 20 FC models of varying width (from 50–400) and depth (number of hidden layers from 1–5) trained on MNIST. Though the number of native parameters varies by a factor of 24.1, d_{int90} varies by only 1.33, with much of that factor possibly due to noise, showing that d_{int90} is a fairly robust measure across a model family and that extra parameters serve to increase the redundancy of a solution.

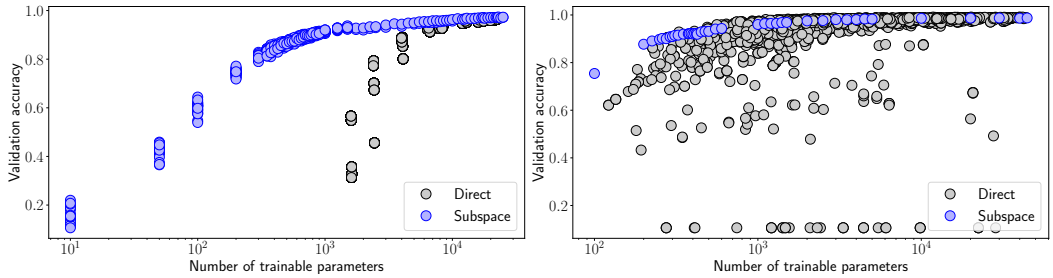

Figure 4: Performance vs. number of trainable parameters for **(left)** FC networks and **(right)** convolutional networks trained on MNIST. Randomly generated direct networks are shown (gray circles) alongside all random subspace training results (blue circles) from the sweep shown in Fig. S6. FC networks show a persistent gap in dimension, suggesting general parameter inefficiency of FC models. Convolutional networks, on the other hand, may be parameter inefficient (gray points significantly to the right of blue manifold) or parameter efficient when well tuned (gray points near blue manifold).

Relationship between Intrinsic Dimension and Minimum Description Length (MDL) As discussed above, the random subspace training method leads naturally to a compressed representation of a network where only d floating point numbers must be stored. We can take this d as a upper bound on the MDL of the problem solution. We cannot yet say the extent to which this bound is loose or tight, but it probably varies by problem. However, to the extent that it is tighter than previous bounds (e.g. just the number of parameters D) and to the extent that it is correlated with the actual MDL, as mentioned by Rissanen (1978) and developed by Hinton & Van Camp (1993), we can use this interpretation to judge which solutions more well-suited to the problem in a principled way. Note that although this approach is related to a rich body of work on estimating the "intrinsic dimension of a dataset" (Camastra & Vinciarelli, 2002; Kégl, 2003; Fukunaga & Olsen, 1971; Levina & Bickel, 2005; Tenenbaum et al., 2000), one must be careful to distinguish between estimating the number of important dimensions of variability in a dataset vs. the number of bits necessary to represent a dataset (related to representing the data distribution, $p(X)$) vs. the number of bits necessary to represent the conditional $p(y|X)$ (as we measure here for supervised models).

Thus, there is some rigor behind our intuitive assumption that we may declare LeNet a *better* model than an FC network for classification on MNIST because its intrinsic dimension is lower (d_{int90} of 275 vs 650). In this particular case this leads to a predictable conclusion, but for the countless less well-studied datasets than MNIST, having a simple method of approximating MDL may prove extremely useful for guiding model exploration.

Table 1: Measured intrinsic dimension d_{int90} on various problems.

Problems	**MNIST**		**MNIST (Shuf Pixels)**		**CIFAR**		**ImageNet**
Network	**MLP**	**LeNet**	**MLP**	**LeNet**	**MLP**	**LeNet**	**SqueezeNet**
Parameter Dim. D	199,210	44,426	199,210	44,426	656,810	62,006	1,248,424
Intrinsic Dim. d_{int90}	650	225	650	750	7.5K	2.5K	$>$ 500K

Are convnets always better on MNIST? Measuring d_{int90} on shuffled data. Zhang et al. (2017) provocatively showed that large networks normally thought to generalize well can nearly as easily be trained to memorize entire training sets with randomly assigned labels or with input pixels provided in random order. Consider two networks: one trained on a real, non-shuffled dataset and an identically sized one trained with shuffled pixels or labels. The networks externally are very similar: the training loss may even be identical at the final epoch. However, the intrinsic dimension of each may be measured to expose the differences in problem difficulty. When training on a dataset of **shuffled pixels**, the intrinsic dimension of an FC network remains the same at 650 (as it must). But the intrinsic dimension of a convnet increases from 250 to 750 — even higher than a fully connected network. While convnets are better suited to classifying digits given images with natural, local structure, when this structure is removed, violating convolutional assumptions, we can measure that the model's inappropriate assumptions now require even more degrees of freedom to model the underlying distribution. When training on MNIST with **shuffled labels**, we redefine our measure of d_{int90} relative to training accuracy, as validation accuracy necessarily remains at chance. We find to memorize random labels on the MNIST dataset requires a very high dimension, $d_{\text{int90}} = 190,000$, or 3.8 floats per memorized label. Sec. S5.3 gives a few further results, in particular that the more labels are memorized, the more efficient memorization is (in terms of floats per label). Thus while generalization performance to an unseen validation set is still obviously 0, "generalization" *within* a training set may occur as networks build shared infrastructure for memorizing labels.

3.2 CIFAR-10 AND IMAGENET

We run further experiments on CIFAR-10 and ImageNet. When attempting to scale beyond MNIST-sized networks — those with D on the order of 200k and d on the order of 1k — we find it necessary to use more efficient methods of generating and projecting from random subspaces. In the case of ImageNet the situation is even severer, as the direct network can easily go beyond millions of parameters. In Sec. S7, we describe and characterize scaling properties of three methods of projection: dense matrix projection, sparse matrix projection (Li et al., 2006), and the beautifully efficient Fastfood transform (Le et al., 2013). To train networks on CIFAR we generally use the sparse projection method, and for ImageNet we employ the Fastfood transform.

Full results on CIFAR10 are given in Sec. S8, and ImageNet in Sec. S9. Measured d_{int90} values are given in Table 1. To summarize, for CIFAR-10 we find qualitatively similar results to MNIST, but with generally higher dimension (7.5k vs. 650 for MLP and 2.5k vs 225 for convnets). Due to deadline pressures and memory issues, training on ImageNet has not yet given a reliable estimate for d_{int90} except that it is over 500k.

3.3 REINFORCEMENT LEARNING ENVIRONMENTS

Measuring intrinsic dimension allows us to perform some comparison across the divide between supervised learning and reinforcement learning. Below we measure the intrinsic dimensionality of three control tasks of varying difficulties using both value-based and policy-based algorithms. The value-based algorithm we evaluate is the Deep Q-Network (DQN) (Mnih et al., 2013), and the policy-based approach is Evolutionary Strategies (ES) (Salimans et al., 2017). Training details are given in Sec. S6.1. For all tasks, performance is defined as the maximum-attained (over training iterations) mean evaluation reward (averaged over 30 evaluations for a given parameter setting). The solid points in the plots correspond to the (noisy) median observed performance value for runs with a given d, and the uncertainty intervals give the maximum and minimum performance values observed. The dotted line corresponds to the usual 90% baseline derived from the best directly-trained network.

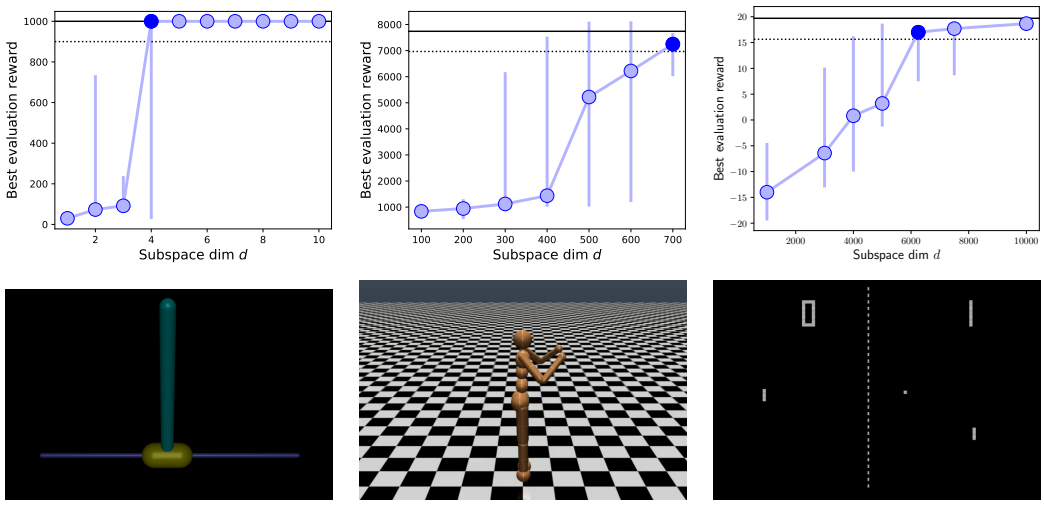

Figure 5: Results using the policy-based Evolutionary Strategies (ES) algorithm to train agents on **(left column)** `InvertedPendulum-v1`, **(middle column)** `Humanoid-v1`, and **(bottom column)** Atari Pong. We find that the inverted pendulum task is surprisingly easy, with $d_{\text{int100}} = d_{\text{int90}} = 4$, meaning that only four parameters are needed to solve the problem, in this case perfectly (see Stanley & Miikkulainen (2002) for a similarly small solution found via evolution). The walking humanoid task is more difficult, but solutions are found reliably by dimension 700, or with about as much complexity as required as modeling MNIST with a fully connected network, and far less than modeling CIFAR-10 with a convnet. Finally, to play Pong on Atari (directly from pixels) requires a network trained in a 6k subspace, making it roughly on the order of modeling CIFAR-10.

We give basic results for three tasks — `InvertedPendulum-v1`, `Humanoid-v1`, and Atari Pong — trained using ES in Fig. 5, with more complete ES results in Sec. S6.2, and results for DQN in Sec. S6.3.

4 Conclusions and Future Directions

We have defined the intrinsic dimension of optimization problems and shown a simple method — random subspace training — of approximating it for neural network modeling problems. We find in some cases intrinsic dimensions much lower than the direct parameter dimension, which enables effective network compression, and in other cases intrinsic dimension similar to that of the best tuned models, which endorses those models as well-suited to the problem. In cases where intrinsic dimension is far smaller than the direct dimension, future work could investigate using much more powerful solvers — e.g. more expensive second order methods — due to the parsimonious parameter length. Recent promising attempts to solve catastrophic forgetting like Elastic Weight Consolidation (EWC) (Kirkpatrick et al., 2017) have relied on annotating individual parameters in a network with their relative importance; training in random subspaces yields directly a subspace that matters and the dimension — though not orientation — of the subspace that does not, which could enable networks that forget less. Further work could also identify better ways of creating subspaces for reparameterization: here we chose random linear subspaces, but one might carefully construct linear or non-linear subspaces to be even more efficient, or pre-scale or otherwise transform the direct parameters before projecting to or from the subspace to make projections more likely to intersect solutions. Finally, as the field departs from single stack-of-layers image classification models toward larger and more heterogeneous networks (Ren et al., 2015; Kaiser et al., 2017) often composed of many modules and trained by many losses, methods — like measuring intrinsic dimension — that allow some automatic assessment of model components might provide much-needed greater understanding of individual black-box module properties.

Acknowledgments

[Removed for blind review.]

REFERENCES

Greg Brockman, Vicki Cheung, Ludwig Pettersson, Jonas Schneider, John Schulman, Jie Tang, and Wojciech Zaremba. Openai gym, 2016.

Francesco Camastra and Alessandro Vinciarelli. Estimating the intrinsic dimension of data with a fractal-based method. *IEEE Transactions on pattern analysis and machine intelligence*, 24(10): 1404–1407, 2002.

Yann Dauphin and Yoshua Bengio. Big neural networks waste capacity. *CoRR*, abs/1301.3583, 2013. URL http://arxiv.org/abs/1301.3583.

Yann Dauphin, Razvan Pascanu, Çaglar Gülçehre, Kyunghyun Cho, Surya Ganguli, and Yoshua Bengio. Identifying and attacking the saddle point problem in high-dimensional non-convex optimization. *CoRR*, abs/1406.2572, 2014. URL http://arxiv.org/abs/1406.2572.

Misha Denil, Babak Shakibi, Laurent Dinh, Nando de Freitas, et al. Predicting parameters in deep learning. In *Advances in Neural Information Processing Systems*, pp. 2148–2156, 2013.

Keinosuke Fukunaga and David R Olsen. An algorithm for finding intrinsic dimensionality of data. *IEEE Transactions on Computers*, 100(2):176–183, 1971.

Xavier Glorot and Yoshua Bengio. Understanding the difficulty of training deep feedforward neural networks. In *Artificial Intelligence and Statistics*, 2010.

Ian J. Goodfellow, Oriol Vinyals, and Andrew M. Saxe. Qualitatively characterizing neural network optimization problems. In *International Conference on Learning Representations (ICLR 2015)*, 2015. URL http://arxiv.org/abs/1412.6544.

Song Han, Huizi Mao, and William J Dally. Deep compression: Compressing deep neural networks with pruning, trained quantization and huffman coding. *ICLR*, 2016.

Kaiming He, Xiangyu Zhang, Shaoqing Ren, and Jian Sun. Delving deep into rectifiers: Surpassing human-level performance on imagenet classification. In *CVPR*, 2015.

Geoffrey E Hinton and Drew Van Camp. Keeping neural networks simple by minimizing the description length of the weights. In *Proceedings of the sixth annual conference on Computational learning theory*, pp. 5–13. ACM, 1993.

Forrest N Iandola, Song Han, Matthew W Moskewicz, Khalid Ashraf, William J Dally, and Kurt Keutzer. Squeezenet: Alexnet-level accuracy with 50x fewer parameters and¡ 0.5 mb model size. *arXiv preprint arXiv:1602.07360*, 2016.

Lukasz Kaiser, Aidan N. Gomez, Noam Shazeer, Ashish Vaswani, Niki Parmar, Llion Jones, and Jakob Uszkoreit. One model to learn them all. *CoRR*, abs/1706.05137, 2017. URL http://arxiv.org/abs/1706.05137.

Balázs Kégl. Intrinsic dimension estimation using packing numbers. In *Advances in neural information processing systems*, pp. 697–704, 2003.

Diederik Kingma and Jimmy Ba. Adam: A method for stochastic optimization. *arXiv preprint arXiv:1412.6980*, 2014.

James Kirkpatrick, Razvan Pascanu, Neil Rabinowitz, Joel Veness, Guillaume Desjardins, Andrei A. Rusu, Kieran Milan, John Quan, Tiago Ramalho, Agnieszka Grabska-Barwinska, Demis Hassabis, Claudia Clopath, Dharshan Kumaran, and Raia Hadsell. Overcoming catastrophic forgetting in neural networks. *Proceedings of the National Academy of Sciences*, 114(13):3521–3526, 2017. doi: 10.1073/pnas.1611835114. URL http://www.pnas.org/content/114/13/3521.abstract.

Quoc Le, Tamás Sarlós, and Alex Smola. Fastfood-approximating kernel expansions in loglinear time. In *ICML*, 2013.

Elizaveta Levina and Peter J Bickel. Maximum likelihood estimation of intrinsic dimension. In *Advances in neural information processing systems*, pp. 777–784, 2005.

Ping Li, T. Hastie, and K. W. Church. Very sparse random projections. In *KDD*, 2006.

C. Louizos, K. Ullrich, and M. Welling. Bayesian Compression for Deep Learning. *ArXiv e-prints*, May 2017.

V. Mnih, K. Kavukcuoglu, D. Silver, A. Graves, I. Antonoglou, D. Wierstra, and M. Riedmiller. Playing Atari with Deep Reinforcement Learning. *ArXiv e-prints*, December 2013.

Shaoqing Ren, Kaiming He, Ross Girshick, and Jian Sun. Faster r-cnn: Towards real-time object detection with region proposal networks. In *Advances in neural information processing systems*, pp. 91–99, 2015.

Jorma Rissanen. Modeling by shortest data description. *Automatica*, 14(5):465–471, 1978.

T. Salimans, J. Ho, X. Chen, and I. Sutskever. Evolution Strategies as a Scalable Alternative to Reinforcement Learning. *ArXiv e-prints*, March 2017.

Kenneth Stanley and Risto Miikkulainen. Evolving neural networks through augmenting topologies. *Evolutionary computation*, 10(2):99–127, 2002.

Joshua B Tenenbaum, Vin De Silva, and John C Langford. A global geometric framework for nonlinear dimensionality reduction. *science*, 290(5500):2319–2323, 2000.

Tijmen Tieleman and Geoffrey Hinton. Lecture 6.5-rmsprop: Divide the gradient by a running average of its recent magnitude. *COURSERA: Neural networks for machine learning*, 4(2):26–31, 2012.

Emanuel Todorov, Tom Erez, and Yuval Tassa. Mujoco: A physics engine for model-based control. In *Intelligent Robots and Systems (IROS), 2012 IEEE/RSJ International Conference on*, pp. 5026–5033. IEEE, 2012.

Wei Wen, Chunpeng Wu, Yandan Wang, Yiran Chen, and Hai Li. Learning structured sparsity in deep neural networks. In *NIPS*, 2016.

Zichao Yang, Marcin Moczulski, Misha Denil, Nando de Freitas, Alex Smola, Le Song, and Ziyu Wang. Deep fried convnets. In *Proceedings of the IEEE International Conference on Computer Vision*, pp. 1476–1483, 2015.

Chiyuan Zhang, Samy Bengio, Moritz Hardt, Benjamin Recht, and Oriol Vinyals. Understanding deep learning requires rethinking generalization. *ICLR*, 2017.

Supplementary Information for: Measuring the Intrinsic Dimension of Objective Landscapes

S5 Additional MNIST results

S5.1 Results for all 20 FC networks

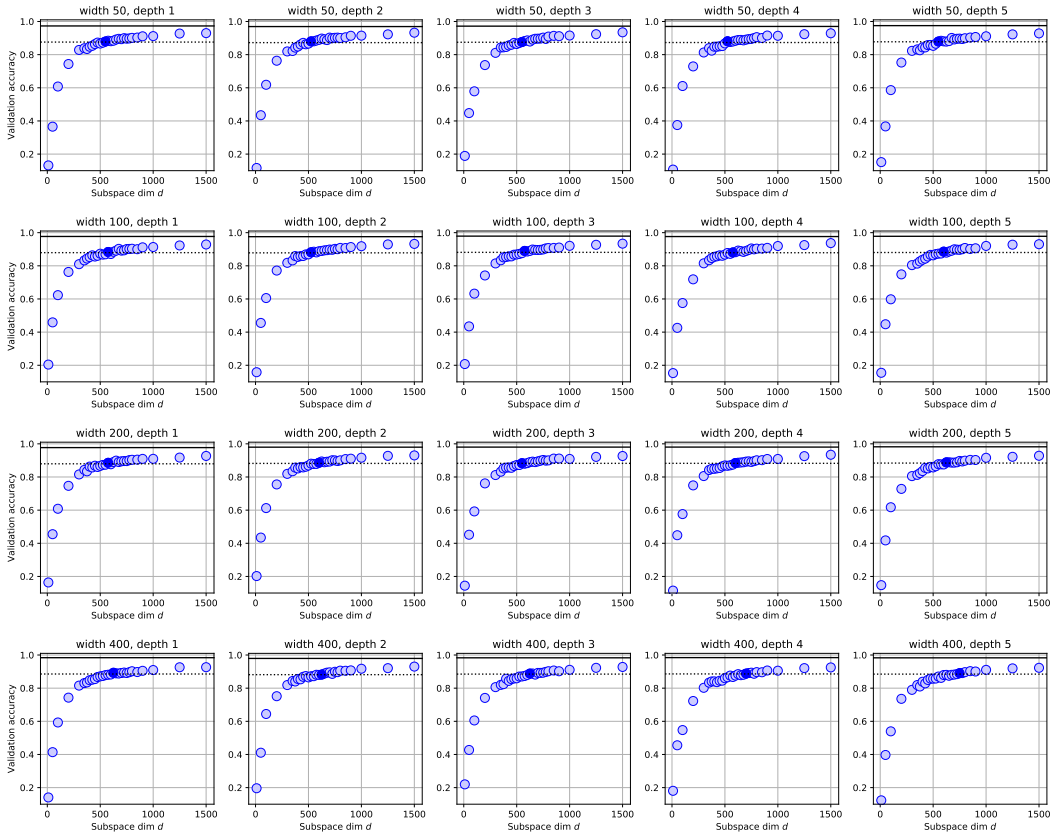

Figure S6: MNIST FC network: validation accuracy vs subspace dimension for a sweep over network depth and width. Number of hidden layers chosen from {1,2,3,4,5} and width of each hidden layer chosen from {50,100,200,400}.

S5.2 Training stability

A minor but interesting result is that random subspace training can in some cases make optimization more stable. Fig. S8 shows training results for FC networks with up to 10 layers. SGD with step 0.1, and ReLUs with He initialization is used. Multiple networks failed at depths 4, and all failed at depths higher than 4, despite and activiation function and initialization designed to make learning stable (He et al., 2015). Because each random basis vector projects across all D direct parameters, the optimization problem may be far better conditioned. A related potential downside is that projecting the D parameters which may have widely varying scale could result in ignoring parameter dimensions with tiny gradients. This situation is similar to that faced by methods like SGD, but ameliorated by RMSProp, Adam, and other methods that can rescale individual step sizes to account for individual parameter scales. Though convergence seems robust, further work may

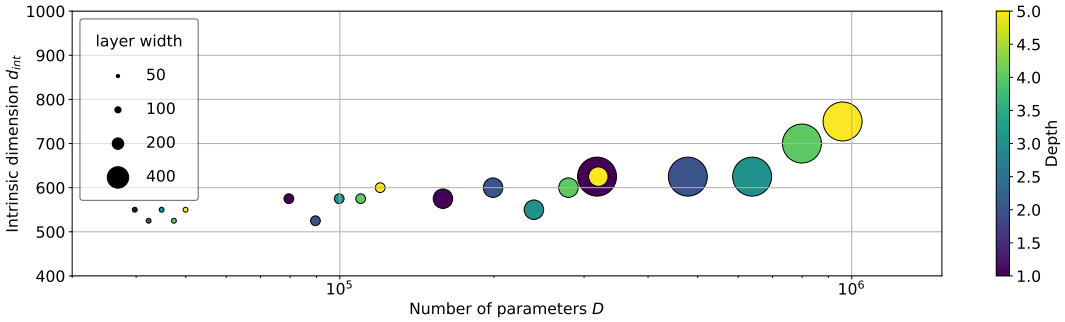

Figure S7: Measured intrinsic dimension d_{int90} vs number of parameters D for 20 models of varying width (from 50 - 400) and depth (number of hidden layers from 1-5) trained on MNIST. As opposed to Fig. 3, which used a global, shared baseline across all models, here a per-model baseline is used. The number of native parameters varies by a factor of 24.1, but d_{int90} varies by only 1.42. The per-model baseline results in higher measured d_{int90} for larger models because they have a higher baseline performance than the shallower models.

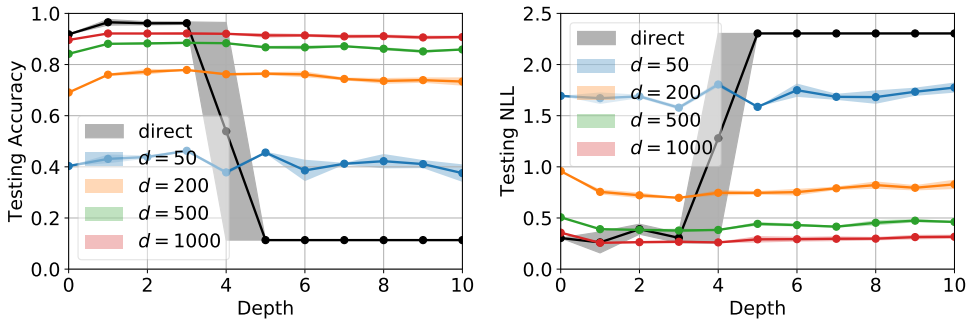

(a) Accuracy

(b) Negative Log Likelihood (NLL)

Figure S8: Results of subspace training versus the number of layers in a fully connected network trained on MNIST. The direct method always fail to converge when $L > 5$, while our subspace training yields stable performance across depths.

be needed to improve network amenability to subspace training: for example by ensuring direct parameters are similarly scaled by clever construction or by inserting a pre-scaling layer between the projected subspace and the direct parameters themselves.

S5.3 Additional shuffled label results

The $d_{\text{int90}} = 190,000$ result mentioned in the main text holds for the full MNIST dataset (50k examples). We can interpret this as requiring 3.8 floats to memorize each random label (at 90% accuracy). Curious how this scales with dataset size, we estimated d_{int90} on shuffled label versions of MNIST at different scales and found fairly interesting results, shown in Table S2 and Fig. S9. As the dataset memorized becomes smaller, the number of floats required to memorize each label becomes larger. The best interpretation is not yet clear, but one possible interpretation is that networks required to memorize large training sets make use of shared machinery for memorization. In other words, though generalization performance to a validation set is still obviously 0, generalization *within* a training set is non-negligible.

Fraction of MNIST training set	$d_{\text{int}}90$	floats per label
100%	190k	3.8
50%	130k	5.2
10%	90k	18.0

Table S2: d_{int90} measured on a dataset memorization task with different dataset sizes

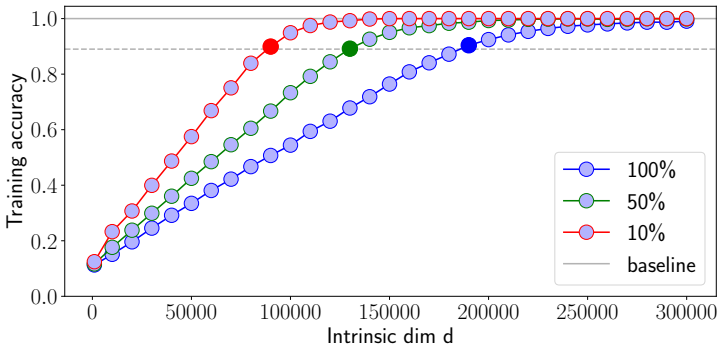

Figure S9: Training accuracy of MLP ($W = 400$, $L = 5$) with different subspace dimension d on 100%, 50%, 10% data of shuffled label version of MNIST.

We trained the same size MNIST network that above had $d_{\text{int90}} = 850$ on a version of MNIST with shuffled labels. 10%, 50%, 100% of the dataset was tested, and d_{int90} increased to 90k, 130k, and 190k, respectively (see Fig. S9). This is consistent with our intuition that the problem becomes harder, as more "random pairs" are required to memorize via the neural networks.

Interestingly, for MNIST with shuffled labels, it is very difficult to reach high training accuracy using direct training method. However, subspace training is stable to excellent performance as d increases.

S5.4 The role of optimizers

We investigate the impact of stochastic optimization methods on the intrinisc dimension, using MLPs on standard MNIST dataset. Two classic optimizers are used: SGD (0.1) and Adam (0.001). The intrinsic dimension d_{int90} are reported in Figure S15 (a) (b).

S6 Additional Reinforcement Learning results and details

S6.1 ES Training Details

We've included the hyperparmeters used in training the three RL tasks using ES in Table S3.

	ℓ_2 penalty	Adam LR	ES σ	Iterations
`InvertedPendulum-v1`	1×10^{-8}	3×10^{-1}	2×10^{-2}	1000
`Humanoid-v1`	5×10^{-3}	3×10^{-2}	2×10^{-2}	2000
`Pong-v0`	5×10^{-3}	3×10^{-2}	2×10^{-2}	500

Table S3: Hyperparameters used in training RL tasks using ES. σ refers to the parameter perturbation noise used in ES. Default Adam parameters of $\beta_1 = 0.9$, $\beta_2 = 0.999$, $\epsilon = 1 \times 10^{-7}$ were used.

S6.2 ES Complete Results

S6.2.1 Inverted Pendulum

The `InvertedPendulum-v1` environment uses the MuJoCo physics simulator (Todorov et al., 2012) to instantiate the same problem as `CartPole-v0` in a realistic setting. We expect that even with more accurate environment dynamics, as well as a different RL algorithm – evolutionary strategies (ES) – the intrinsic dimensionality should be similar. As seen in Fig. 5, the measured intrinsic dimensionality $d_{\text{int90}} = 4$ is of the same order of magnitude, but smaller. Interestingly, although the environment dynamics are more complex than in `CartPole-v0`, using ES rather than DQN seems to induce a simpler objective landscape.

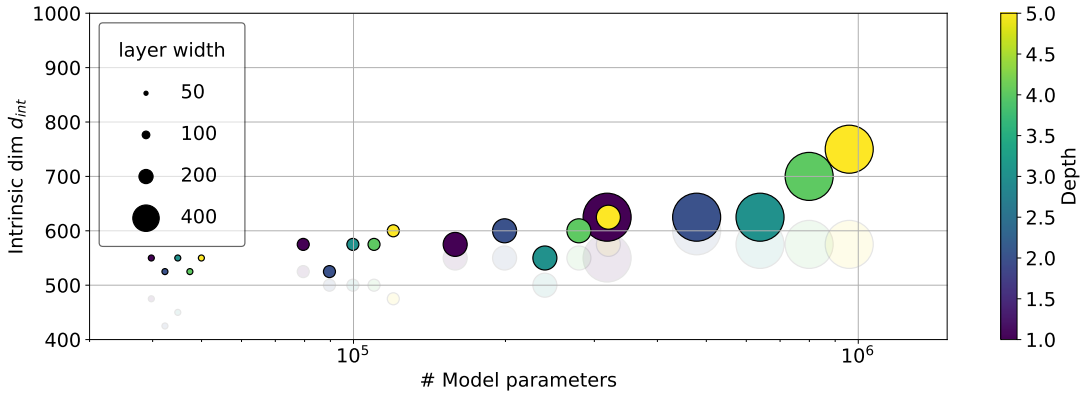

(a) Global baseline

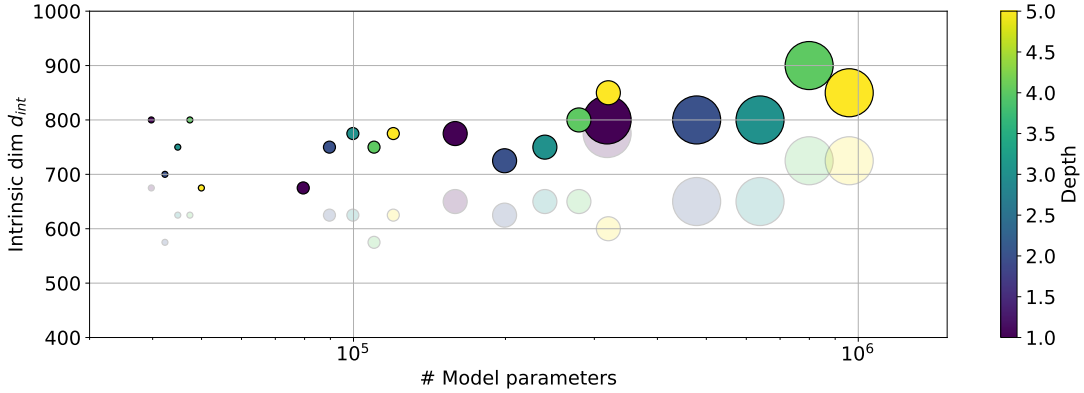

(b) Individual baseline

Figure S10: The role of optimizers. The transparent dots indicate SGD results, and solid dots indicate Adam results.

S6.2.2 Learning to walk

A more challenging problem is `Humanoid-v1`, also using the MuJoCo simulator. Intuitively, one might believe that learning to walk is a more complex task than classifying images. Our results show the contrary – that the learned intrinsic dimensionality of $d_{\text{int90}} = 700$ is similar to that of MNIST on a fully-connected network ($d_{\text{int90}} = 650$) but significantly less than that of even a convnet trained on CIFAR10 ($d_{\text{int90}} = 2,500$). Fig. 5 shows the full results. Interestingly, we begin to see training runs reach the threshold as early as $d = 400$, with the median performance steadily increasing with d.

S6.2.3 Atari Pong

Finally, using a base convnet of approximately $D = 1M$ in the `Pong-v0` pixels-to-actions environment (using 4-frame stacking), we were able to determine $d_{\text{int90}} = 6,000$.

S6.3 DQN experiments

DQN on Cartpole We start with a simple classic control game `CartPole-v0` in OpenAI Gym (Brockman et al., 2016). The full game ends when one of two failure conditions is satisfied: the cart moves more than 2.4 units from the center, or the pole is more than 15 degrees from vertical. The system is controlled by applying a force of left or right to the cart. The pendulum starts upright, and the goal is to prevent it from falling over. A reward of +1 is provided for every timestep. We created two potentially easier environments called `Pole` and `Cart`, by removing one of failure conditions respectively. DQN is used, where the value netwowrk is parameterized by an MLP ($L = 2, W = 400$). Five runs are tested for each subspace d, the mean is used to computed d_{int90},

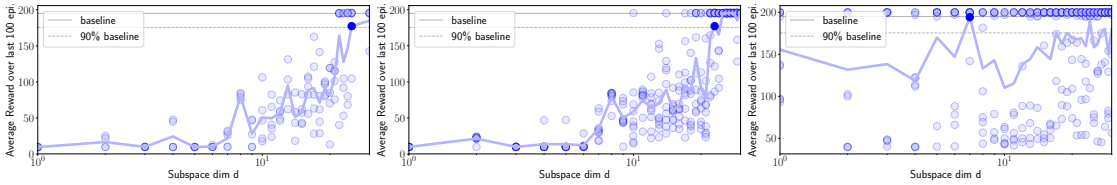

(a) CartPole ($d_{\text{int90}} = 25$) (b) Pole ($d_{\text{int90}} = 23$) (c) Cart ($d_{\text{int90}} = 7$)

Figure S11: Average reward of 3 CartPole environments using DQN.

where the baseline is set as 195.0[4]. The results are shown in Figure S11. The intrinsic dimension for CartPole, Pole and Cart is $d_{\text{int90}} = 25, 23, 7$, respectively. It quantifies the difficulty of each part of the full game: driving a cart in a given interval is much easier than keeping a pole straight.

S7 THREE METHODS OF RANDOM PROJECTION

Scaling the random subspace training procedure to large problems requires an efficient way to map from $\mathbb{R}^d$ into a random d-dimensional subspace of $\mathbb{R}^D$ that does not necessarily include the origin. Algebraically, we need to left-multiply a vector of parameters $v \in \mathbb{R}^d$ by a random matrix $M \in \mathbb{R}^{D \times d}$, whose columns are orthonormal, then add an offset vector $\theta_0 \in \mathbb{R}^D$. If the low-dimensional parameter vector in $\mathbb{R}^d$ is initialized to zero, then specifying an offset vector is equivalent to choosing an initialization point in the original model parameter space $\mathbb{R}^D$.

A naïve approach to generating the random matrix M is to use a dense $D \times d$ matrix of independent standard normal entries, then scale each column to be of length 1. The columns will be approximately orthogonal if D is large because of the independence of the entries. Although this approach is sufficient for low-rank training of models with few parameters, we quickly run into scaling limits because both matrix-vector multiply time and storage of the matrix scale according to $\mathcal{O}(Dd)$. We were able to successfully determine the intrinsic dimensionality of MNIST (d=225) using a LeNet (D=44,426), but were unable to increase d beyond 1,000 when applying a LeNet (D=62,006) to CIFAR10, which did not meet the performance criterion to be considered the problems intrinsic dimensionality.

Random matrices need not be dense for their columns to be approximately orthonormal. In fact, a method exists for "very sparse" random projections (Li et al., 2006), which achieves a density of $\frac{1}{\sqrt{D}}$. To construct the $D \times d$ matrix, each entry is chosen to be nonzero with probability $\frac{1}{\sqrt{D}}$. If chosen, then with equal probability, the entry is either positive or negative with the same magnitude in either case. The density of $\frac{1}{\sqrt{D}}$ implies $\sqrt{D}d$ nonzero entries, or $\mathcal{O}(\sqrt{D}d)$ time and space complexity. Implementing this procedure allowed us to find the intrinsic dimension of d=2,500 for CIFAR10 using a LeNet mentioned above. Unfortunately, when using Tensorflow's `SparseTensor` implementation we did not achieve the theoretical $\sqrt{D}$-factor improvement in time complexity (closer to a constant 10x). Nonzero elements also have a significant memory footprint of 24 bytes, so we could not scale to larger problems with millions of model parameters and large intrinsic dimensionalities.

We need not explicitly form and store the transformation matrix. The Fastfood transform (Le et al., 2013) was initially developed as an efficient way to compute a nonlinear, high-dimensional feature map $\phi(x)$ for a vector x. A portion of the procedure involves implicitly generating a $D \times d$ matrix with approximately uncorrelated standard normal entries, using only $\mathcal{O}(D)$ space, which can be multiplied by v in $\mathcal{O}(D \log d)$ time using a specialized method. The method relies on the fact that Hadamard matrices multiplied by Gaussian vectors behave like dense Gaussian matrices. In detail, to implicitly multiply v by a random *square* Gaussian matrix M with side-lengths equal to a power of two, the matrix is factorized into multiple simple matrices: $M = HG\Pi HB$, where B is a random diagonal matrix with entries +-1 with equal probability, H is a Hadamard matrix, Π is a random permutation matrix, and G is a random diagonal matrix with independent standard normal entries. Multiplication by a Hadamard matrix can be done via the Fast Walsh-Hadamard Transform in $\mathcal{O}(d \log d)$ time and takes no additional space. The other matrices have linear time and space

[4] `CartPole-v0` is considered as "solved" when the average reward over the last 100 episodes is 195

complexities. When $D > d$, multiple independent samples of M can be stacked to increase the output dimensionality. When d is not a power of two, we can zero-pad v appropriately. Stacking $\frac{D}{d}$ samples of M results in an overall time complexity of $\mathcal{O}(\frac{D}{d} d \log d) = \mathcal{O}(D \log d)$, and a space complexity of $\mathcal{O}(\frac{D}{d} d) = \mathcal{O}(D)$. In practice, the reduction in space footprint allowed us to scale to much larger problems, including the Pong RL task using a 1M parameter convolutional network for the policy function.

Table S4 summarizes the performance of each of the three methods theoretically and empirically.

	Time complexity	Space complexity	D = 100k	D = 1M	D = 60M
Dense	$\mathcal{O}(Dd)$	$\mathcal{O}(Dd)$	0.0169 s	1.0742 s*	4399.1 s*
Sparse	$\mathcal{O}(\sqrt{D}d)$	$\mathcal{O}(\sqrt{D}d)$	0.0002 s	0.0019 s	0.5307 s*
Fastfood	$\mathcal{O}(D \log d)$	$\mathcal{O}(D)$	0.0181 s	0.0195 s	0.7949 s

Table S4: Comparison of theoretical complexity and average duration of a forward+backward pass through M (in seconds). d was fixed to 1% of D in each measurement. D = 100k is approximately the size of an MNIST fully-connected network, and D = 60M is approximately the size of AlexNet. The Fastfood timings are based on a Tensorflow implementation of the Fast Walsh-Hadamard Transform, and could be drastically reduced with an efficient CUDA implementation. Asterisks mean that we encountered an out-of-memory error, and the values are extrapolated from the largest successful run (a few powers of two smaller). For example, we expect sparse to outperform Fastfood if it didn't run into memory issues.

S8 Additional CIFAR-10 Results

We consider the CIFAR10 dataset, and test the same set of MLP and LeNet architecure as on MNIST. For MLP, d_{int90} values for all 20 networks are shown in S13 (a) plotted against the native dimension D of each network; D changes by a factor of 12.16 between the smallest and largest networks, but d_{int90} changes over this range by a factor of 5.0. In S13 (b), we also compute the intrinsic dimension wrt to a global baseline: 50% validation accuracy, d_{int90} changes over this range by a factor of 1.52. This indicates that various MLPs share similar intrinsic dimension ($d_{\text{int90}} = 5000 \sim 8000$) to achieve the same level of task performance. For LeNet (D=44,426), the validation accuracy vs. subspace dimension d is shown in Fig. S14, the corresponding $d_{\text{int90}} = 2900$. It yields a compression rate of 5%, which is 10 times larger than LeNet on MNIST. It shows that CIFAR images are significantly more difficult to be correctly classified than MNIST. In another word, CIFAR is a harder problem than MNIST, especially given the fact that the notion of "problem solved" (baseline performance) is defined as 99% accuracy on MNIST and 58% accuracy on CIFAR. On the CIFAR dataset, as d increases, subspace training tends to overfitting, we will study the role of subspace training as a regularizer below.

In addition, ResNet exhibits efficient use of parameters with its introduction of residual connections. We are interested to know whether the intrinsic dimension of ResNet on CIFAR is any different. We adopt the smallest 20-layer structure of ResNet with 280K parameters, and find out that it reaches LeNet baseline with $d_{\text{int90}} = 1000 \sim 2000$, while takes a larger d_{int90} $(20,000 \sim 50,000)$ to reach reach its own, much higher baseline.

The role of regularizers We study the effects of weight decay (*i.e.,* ℓ_2 regularizer) on the weights using MLP ($L = 2$, $W = 400$) on CIFAR10 dataset. The amount of weight decay $\lambda = \{10^{-2}, 10^{-3}, 10^{-4}, 5{\times}10^{-4}, 10^{-5}, 0\}$. The testing accuracy and negative log-likelihood (NLL) are reported in Figure S15 (a) (b), respectively. As expected, larger amount of weight decay reduces the gap between training and testing for both direct and our subspace training methods. Interestingly, our procedure exhibits strong regularization ability, especially when d is small. It outperforms direct method in terms of testing accuracy when d is properly chosen, suggesting the potential of this method as a beteter alternative to traditional weight decay. When d is large, the method also overfits the training dataset.

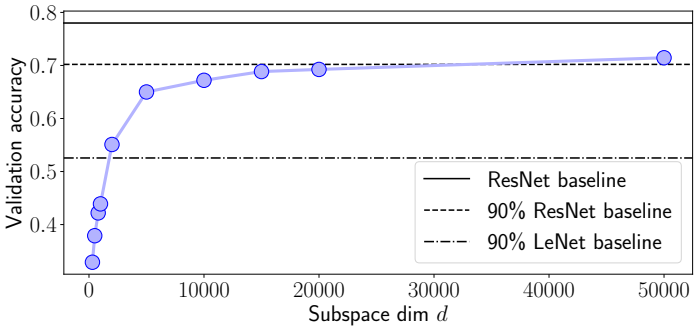

Figure S12: Validation accuracy of ResNet on CIFAR with different subspace dimension d. It surpasses the 90% baseline on LeNet at d between 1000 and 2000, 90% of ResNet baseline between 20k and 50k.

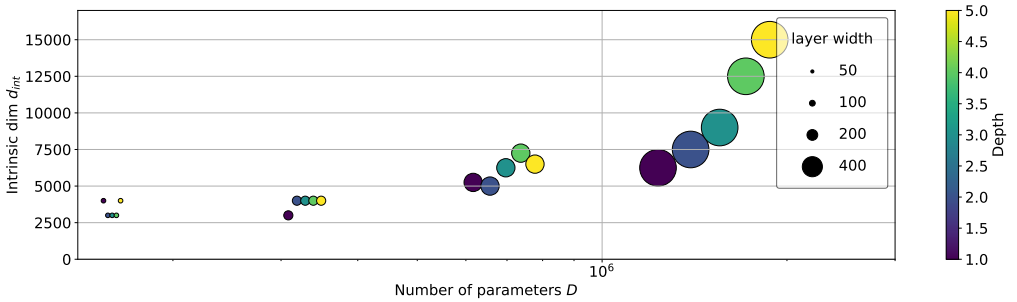

(b) Individual baseline

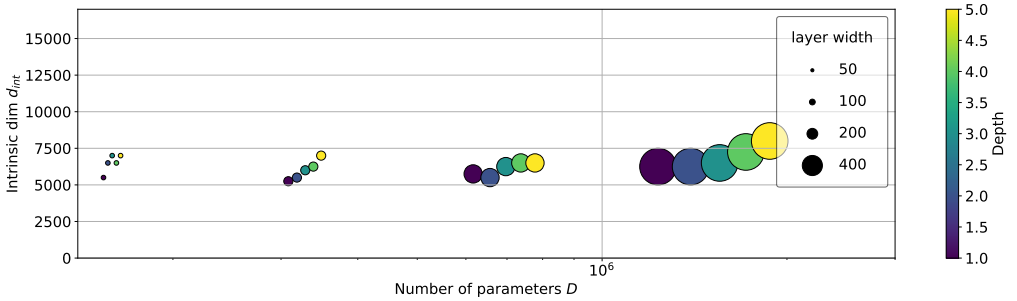

(a) Global baseline

Figure S13: Intrinsic dimension of MLP with various width and depth on CIFAR 10 dataset.

S9 IMAGENET

To investigate the applicability of our proposed method to large-scale problems, we take on ImageNet classification. A relatively smaller network, SqueezeNet by Iandola et al. (2016), of parameter size 1.24M, is used. A direct training produces Top-1 accuracy of 55.5%. We vary intrinsic dimension from 300 to 500K, and record the validation accuracies as shown in Fig. S14. The training of each intrinsic dimension takes about 6 to 7 days, while distributed among 4 GPUs.

S10 SUMMARIZATION OF d_{int90}

We summarize d_{int90} for all the experiments in Table S5.

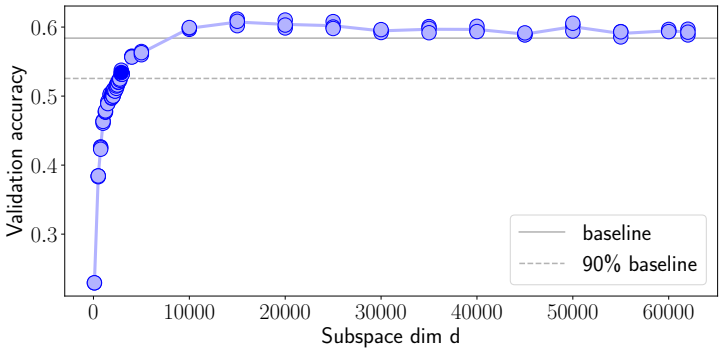

Figure S14: Validation accuracy of LeNet with different subspace dimension d on CIFAR10.

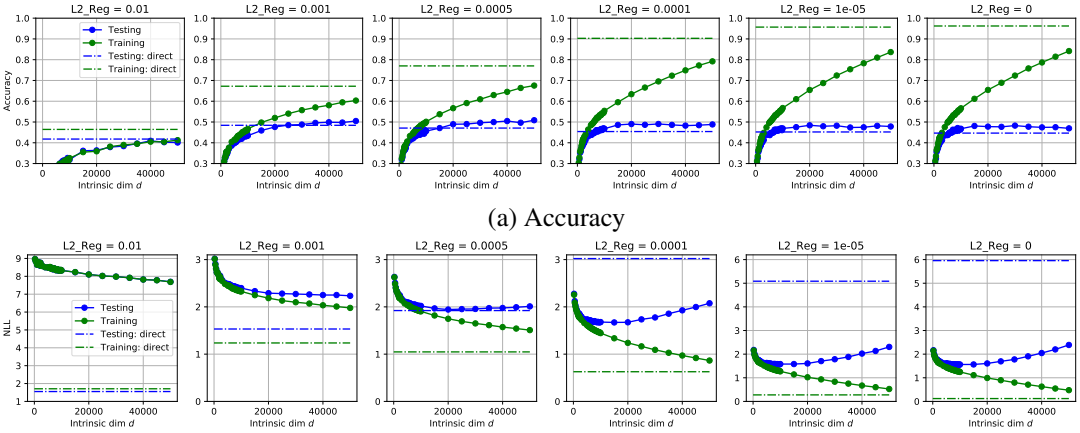

(a) Accuracy

(b) Negative Log Likelihood (NLL)

Figure S15: Comparing regularization induced by an L2 penalty with that induced from training in reduced subspace.

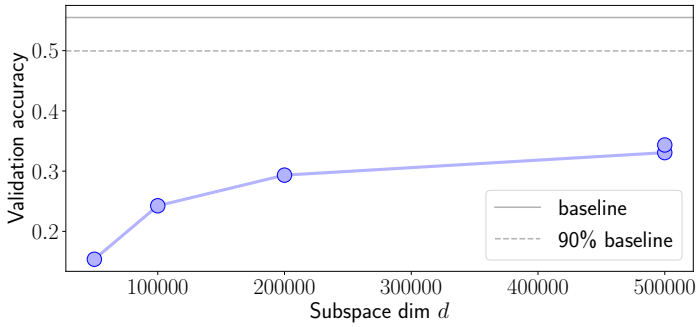

Figure S16: Validation accuracy of SqueezeNet on ImageNet with different subspace dimension d. At $d = 500k$ the accuracy reaches 34.34%, which is not yet past the threshold required to estimate d_{int90}.

Table S5: Summary of measured intrinsic dimension values. "PP" indicates permuted pixel, and "PL" for permuted label, and "MLP-5" for a 5-layer MLP.

Dataset	Network	D	d_{int90}
MNIST	MLP	199210	750
MNIST	LeNet	44426	275
Cifar	MLP	1393610	8000
Cifar	LeNet	62006	2900
MNIST-PP	MLP	199210	750
MNIST-PP	LeNet	44426	750
MNIST-PL-100%	MLP-5	959610	190000
MNIST-PL-50%	MLP-5	959610	130000
MNIST-PL-10%	MLP-5	959610	90000
MNIST	Untied-LeNet	286334	600
MNIST	MLP-LeNet	3640574	2000
Cifar	Untied-LeNet	658238	9000
Cifar	MLP-LeNet	16397726	$>$100000
ImageNet	SqueezeNet	124842	$>$500000
CartPole	MLP	199210	25
Pole	MLP	199210	23
Cart	MLP	199210	9
InvertedPendulum	MLP	562	4
Humanoid	MLP	166673	700
Atari Pong	ConvNet	1005974	6000